

OPTIMIZATION OF BBr₃ DIFFUSION PROCESSES FOR N-TYPE SILICON SOLAR CELLS

S. Werner¹, E. Lohmüller¹, U. Belledin¹, A.H.G. Vlooswijk², R.C.G. Naber², S. Mack¹, A. Wolf¹

¹Fraunhofer Institute for Solar Energy Systems ISE, Heidenhofstraße 2, 79110 Freiburg, Germany

²Tempress Systems, Radeweg 31, 8171 MD Vaassen, The Netherlands

Phone: +49 761 4588 5049, e-mail: sabrina.werner@ise.fraunhofer.de

ABSTRACT: In this work, we investigate boron diffusion processes for emitter formation on the front side of n-type Cz-Si solar cells with an edge length of 156 mm. The processes are performed in an industrial tube furnace from Tempress Systems using boron tribromide (BBr₃) as liquid dopant source. An initial optimization of BBr₃ diffusion processes yields a significant improvement in the homogeneity in sheet resistance R_{sh} across the wafers and from wafer to wafer for full load runs. A standard deviation σ of the R_{sh} across the wafer in the range of 3% is achieved for a mean $R_{sh} \approx 70 \Omega/\text{sq}$. Dark saturation current density $j_{0e} = 60 \text{ fA}/\text{cm}^2$ is extracted from lifetime samples with alkaline textured surface and PECVD Al₂O₃/SiN_x passivation after firing. A second optimization aimed at reducing emitter recombination by decreasing the maximum boron doping concentration N_{max} near the surface. By adapting the post-oxidation incorporated within the BBr₃ diffusion process, N_{max} is decreased to $1.8 \cdot 10^{19} \text{ cm}^{-3}$ while the junction depth increases to slightly above 800 nm ($R_{sh} \approx 115 \Omega/\text{sq}$, σ below 4%). This results in a reduction in j_{0e} to a value of $j_{0e} = 30 \text{ fA}/\text{cm}^2$, which corresponds to an open-circuit voltage limit of 717 mV. Despite the fairly low N_{max} , low specific contact resistance below $4 \text{ m}\Omega\text{cm}^2$ is found for screen-printed and fired contacts using commercially available silver-aluminum paste. Hence, post-oxidation is found to be a promising method for manipulating boron doping profiles while maintaining high homogeneity in R_{sh} .

Keywords: boron, BBr₃, diffusion, oxidation, homogeneity, sheet resistance, n-type, silicon, solar cells.

1 INTRODUCTION

The optimization of boron diffusion processes and the resulting emitter doping profiles are essential for the improvement of n-type silicon solar cells. Typically, the boron-doped emitter is formed by atmospheric pressure tube furnace diffusion processes utilizing boron tribromide (BBr₃) as liquid dopant source.

For homogeneous performance of a solar cell over its full area, the homogeneity of the emitter sheet resistance R_{sh} over the wafer and from wafer to wafer is of major importance. In order to achieve higher open-circuit voltages V_{OC} , the emitter dark saturation current density j_{0e} of the passivated diffused surfaces needs to be decreased. This can for example be realized by reducing the maximum doping concentration N_{max} . Possible approaches to realize this are the implementation of an adapted post-oxidation step in the BBr₃ diffusion process or the performance of a subsequent thermal oxidation. By the use of oxidation, segregation of boron into the growing silicon oxide and oxidation-enhanced diffusion of boron are responsible for lowering N_{max} and an occurring redistribution of the boron dopants [1,2]. However, for usage of such optimized doping profiles on cell level, sufficiently low specific contact resistance ρ_C has to be ensured; using either screen-printed and fired metallization or plated contacts.

Regarding the front side of the solar cell, also the dark saturation current density j_{0met} underneath the metal contacts impacts V_{OC} in addition to j_{0e} of the passivated emitter. One option to reduce the impact of j_{0met} is to increase the junction depth of the boron doping [3].

In this work, three generations of BBr₃ diffusion processes Gen1 to Gen3 are investigated regarding their homogeneity in R_{sh} across wafers with 156 mm edge length. Based on the most homogeneous test-results obtained with process Gen3, its homogeneity from wafer to wafer is also tested for a full load run and process adaptations are performed which aimed at reducing the recombination activity of alkaline textured and passivated boron-doped surfaces by lowering N_{max} . This is realized by adjusting the post-oxidation step following the drive-in phase within the BBr₃ diffusion process.

2 APPROACH

Three generations of BBr₃ diffusion processes Gen1 to Gen3 are provided by *Tempress Systems* and evaluated at *Fraunhofer ISE* utilizing the industrial tube furnace system *TS81255* that features five horizontal quartz tubes. Each quartz boat contains 250 slots for wafers with an edge length of up to 156 mm.

The three process generations feature different process parameters for the deposition and drive-in step. From Gen1 to Gen2, the BBr₃ chemistry is adjusted by changing the gas ratios and the ratio between deposition and drive-in time, while keeping the temperature and total time unchanged. With the transition to Gen3, the temperature of both deposition and drive-in phase is also adjusted. All three diffusion processes feature a short post-oxidation (PO) after the drive-in step at the end of the process sequence to avoid the presence of the highly recombination active boron-rich layer (BRL) at the boron-doped silicon surface after BBr₃ diffusion. To investigate the effect of the PO in more detail, we use a fourth diffusion process Gen3* where process time and process temperature are the same as for process Gen3 but it does not include PO.

After evaluating the three process generations regarding their homogeneity in R_{sh} and emitter recombination activity, and after testing the homogeneity in R_{sh} from wafer to wafer in two full load runs (one with 500 and one with 400 wafers back-to-back with two wafers per slot) for process Gen3, further process variations are performed to reduce N_{max} starting from process Gen3. Therefore, the PO step at the end of the BBr₃ diffusion process is varied. The PO is either extended to the full ramp-down or added to the end of the drive-in step with different durations.

For characterizing the BBr₃ diffusion processes, two sample types are used. The R_{sh} -samples, depicted in Fig. 1(a), allow for measuring R_{sh} and their distribution across the wafer as well as determining depth-dependent boron doping profiles $N(d)$. The j_{0e} samples, illustrated in Fig. 1(b), are utilized to determine j_{0e} of the diffused and passivated alkaline textured surfaces. The fabrication process for both sample types will now be briefly described.

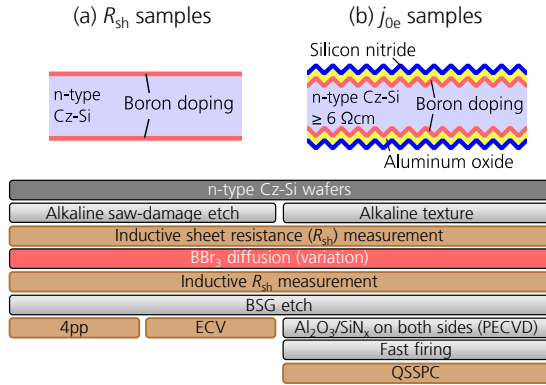


Fig. 1. Schematic cross sections and process sequences of the test samples used to characterize different BBr_3 diffusion processes. The variation in BBr_3 diffusion includes three process generations Gen1 to Gen3 as well as a variation in the PO step based on process Gen3 (4pp: four-point probe, ECV: electrochemical capacitance-voltage, QSSPC: quasi-steady-state photoconductance, PECVD: plasma-enhanced chemical vapor deposition).

2.1 Samples for determining emitter sheet resistances and boron doping profiles

Fig. 1(a) depicts the process sequence for fabrication of the R_{sh} samples to obtain the R_{sh} distributions and boron doping profiles $N(d)$. Following alkaline saw-damage etch of 156 mm n-type Czochralski-grown silicon (Cz-Si) wafers, various BBr_3 diffusion processes are performed and the borosilicate glass (BSG) is etched off using wet chemistry. R_{sh} is measured either by inductive coupling using an inline tool [4] or by the four-point probe (4pp) technique (data measured by 4pp are stated with the subscript “4pp” while data measured by the inductive technique are stated without additional index).

For the inductive measurements, R_{sh} is calculated from the bulk resistance (measured before diffusion; any existing thermal donors have been previously dissolved during a high-temperature step) and the total sheet resistance of the both sides diffused wafer (measured after diffusion). In doing so, a parallel connection of the differently doped layers is assumed. The inductive measurements in this work are performed prior to BSG etch. It is found that the R_{sh} obtained on the same sample once with and once without BSG layer are equal to each other.

The sheet resistance $R_{sh,w}$ of a single wafer w is measured inductively by three sensors s with a diameter of 25 mm and a sensor-to-sensor distance of 52 mm. Every sensor records 36 measurement points p ($R_{sh,s,p}$) on a trace parallel to the wafer edge (see Fig. 2). The mean emitter sheet resistance for a single wafer is calculated using

$$R_{sh,w} = \frac{1}{108} \left(\sum_{s=1}^3 \sum_{p=1}^{36} R_{sh,s,p} \right). \quad (1)$$

The relative standard deviation

$$\sigma_w = \frac{\sqrt{\frac{1}{108} \sum_{s=1}^3 \sum_{p=1}^{36} (R_{sh,s,p} - R_{sh,w})^2}}{R_{sh,w}} \quad (2)$$

is defined as the standard deviation of all measured $R_{sh,s,p}$ of a single wafer relative to the wafer mean emitter sheet resistance $R_{sh,w}$. $R_{sh,w}$ and σ_w are simply named R_{sh} and σ from now on.

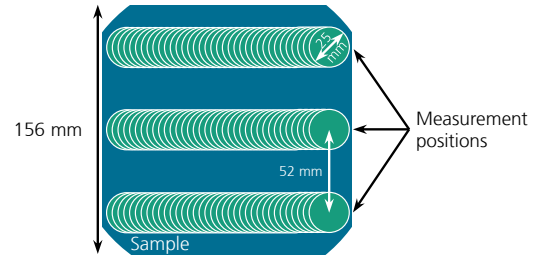


Fig. 2. Pattern of R_{sh} measurement by means of inductive coupling for a sample with 156 mm edge length. The sample moves parallel to the wafer edge over three coils with a diameter of 25 mm each and a distance of 52 mm.

The boron doping profiles are determined by electrochemical capacitance-voltage (ECV) measurements [5] on alkaline saw-damage etched surfaces. Unless otherwise stated, the ECV measurements are performed in the wafer center. The surface area factor is adjusted such that the R_{sh} of the doping profile matches the R_{sh} measured inductively at the ECV measurement spot.

2.2 Samples for determining emitter dark saturation current densities

Alkaline textured n-type Cz-Si lifetime samples with a base resistivity $\rho_B \geq 6 \Omega\text{cm}$ are used to determine emitter dark saturation current densities j_{0e} . The fabrication sequence is depicted in Fig. 1(b). Following BBr_3 diffusion and etching of the BSG layer, a layer stack consisting of aluminum oxide (Al_2O_3) and silicon nitride (SiN_x) is deposited by plasma-enhanced chemical vapor deposition (PECVD) on either side of the wafer. After activating the passivation layers in a co-firing step, quasi-steady-state photoconductance (QSSPC) measurements are performed to extract the j_{0e} values using the latest analysis method introduced by Kimmerle et al. [6].

3 RESULTS

3.1 Homogeneity in emitter sheet resistance for BBr_3 diffusion processes Gen1 to Gen3

Over the three process generations Gen1 to Gen3 for wafers with 156 mm edge length, an improvement in the single wafer's $R_{sh,4pp}$ homogeneity can be seen from the 4pp measurements depicted in Fig. 3, which are performed with a resolution of 20×20 data points. Note that the scaling is different for every $R_{sh,4pp}$ plot. During BBr_3 diffusion the wafers are positioned in the so-called diamond-shape and the upper part of the wafer during diffusion is at the bottom left wafer edge in the figure.

It is clear that the standard deviation σ_{4pp} of $R_{sh,4pp}$ decreases along the different BBr_3 diffusion process generations. Process Gen1 shows the highest $\sigma_{4pp} = 8.8\%$ over the wafer area. Towards process Gen2, σ_{4pp} is considerably decreased to $\sigma_{4pp} = 3.4\%$ while maintaining $R_{sh,4pp} \approx 70 \Omega/\text{sq}$. Further lowering of σ_{4pp} could be achieved with diffusion process Gen3 yielding $\sigma_{4pp} = 2.7\%$. Again, also for process Gen3, the mean $R_{sh,4pp}$ hardly changed. For all three generations, the minimum $R_{sh,4pp}$ found are $\approx 60 \Omega/\text{sq}$, while the maximum values are much higher particularly for Gen1.

A comparison between Gen3 (with PO) and Gen3* (without PO) reveals that the PO shows no effect on the achievable homogeneity in $R_{sh,4pp}$. Only the mean $R_{sh,4pp} = 59 \Omega/\text{sq}$ is lower for Gen3*. The origin of the lower $R_{sh,4pp}$ will be discussed in the next section.

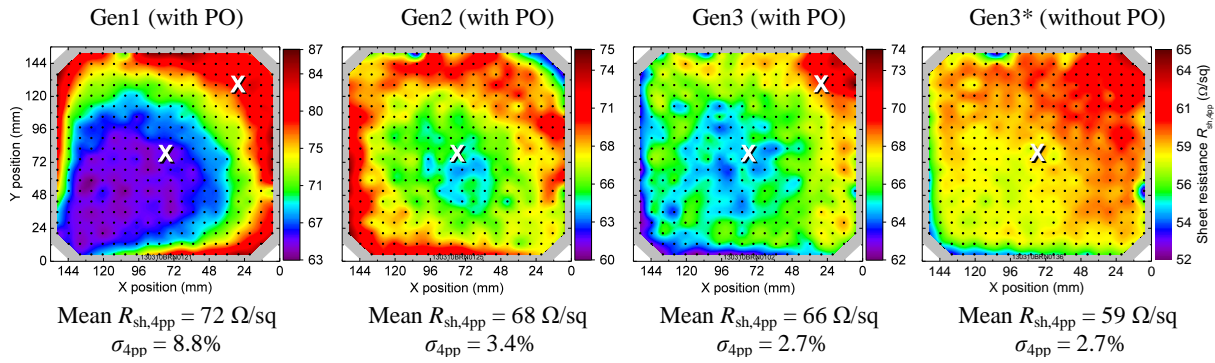


Fig. 3. Four-point probe (4pp) measurements with a 20 x 20 mapping on alkaline saw-damage etched surfaces, where the black dots represent the measurement points (the gray-shaded wafer indicates that the measurements are performed with some distance from the edges). The mean $R_{sh,4pp}$ and the standard deviation σ_{4pp} in $R_{sh,4pp}$ are also stated. Diffusion processes Gen1 to Gen3 feature a post-oxidation (PO) step, while Gen3* does not. “X” marks the positions where ECV measurements are conducted (see Fig. 4 and Fig. 5).

3.2 Boron doping profiles for Gen1 to Gen3

The charge carrier concentration profiles in the samples’ centers determined by ECV measurements for the different generations of BBr₃ diffusion processes are depicted in Fig. 4. The PO step at the end of the diffusion processes Gen1 to Gen3 leads to a pronounced boron depletion at the wafer surface as the solubility of boron is higher in silicon oxide than in silicon [2]. For Gen3* in which no PO step is incorporated, the depletion at the surface is much less pronounced, but the rest of the doping profile equals that of process Gen3. Processes Gen1 and Gen2 show very similar profile progressions with similar N_{max} and depth while Gen3 shows a slightly lower N_{max} and a slightly higher depth.

ECV measurements are also performed at different positions for Gen1 and Gen3 (marked with two “X” symbols in Fig. 3). The selected positions show significant differences in R_{sh} . From the ECV measurements depicted in Fig. 5 it is seen that the distribution in R_{sh} over the wafer surface for process Gen1 correlates with a variation of profile depth and does not correlate with a variation of N_{max} . The doping profiles on both locations have nearly identical N_{max} , but significantly different depths. In contrast, Gen3 yields nearly identical measurements of both N_{max} and depth at the different wafer locations, as this process features very homogeneous boron diffusion.

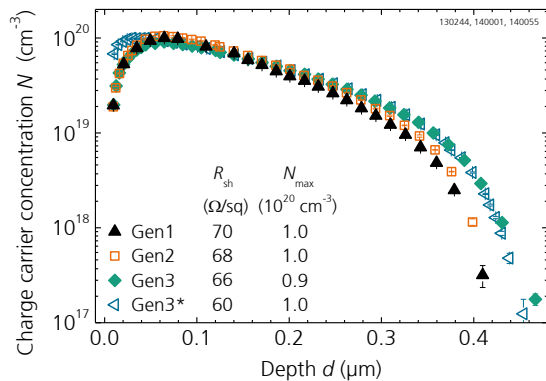


Fig. 4. Charge carrier concentration profiles determined by ECV measurements for the different generations of BBr₃ diffusion processes. The measurements are performed on alkaline saw-damage etched surfaces at the samples’ center positions. The R_{sh} measured by means of inductive coupling at the ECV measurement spots as well as N_{max} are specified.

3.3 Emitter dark saturation current densities for Gen1 to Gen3

The j_{0e} determined from QSSPC measurements on alkaline textured surfaces which are passivated with Al₂O₃/SiN_x layers are specified in Table I. The j_{0e} for Gen1 and Gen2 are at the same level with $j_{0e} \approx 77$ fA/cm², while Gen3 yields a lower $j_{0e} = 60$ fA/cm². Gen3* shows a very high $j_{0e} = 313$ fA/cm². This high j_{0e} originates from a BRL present at the silicon surface, triggering significantly increased charge carrier recombination. As the ECV technique only measures charge carriers, the electrically inactive silicon boride compounds, which are characteristic for a BRL, are not detectable using ECV measurements.

3.4 Process reproducibility of BBr₃ diffusion process Gen3

The industrial high-throughput tube furnace can be loaded by an automated system with 500 wafers back-to-

Table I: Dark saturation current densities j_{0e} of alkaline textured and passivated (PECVD Al₂O₃/SiN_x) samples after firing for the different generations of BBr₃ diffusion processes. The mean j_{0e} are given together with the respective standard deviation of five measurement points over each j_{0e} sample for 2-3 samples per variation.

Diffusion process	Gen1	Gen2	Gen3	Gen3*
j_{0e} (fA/cm ²)	77 ± 5	76 ± 5	60 ± 6	313 ± 111

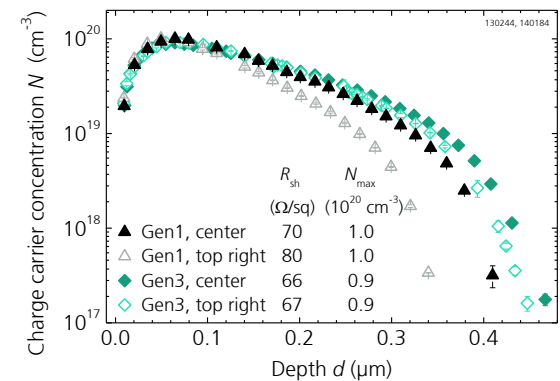


Fig. 5. Charge carrier concentration profiles determined by ECV measurements at the two wafer locations marked in Fig. 3 with different R_{sh} for BBr₃ diffusion processes Gen1 and Gen3. The measurements are performed on alkaline saw-damage etched surfaces. The R_{sh} measured by means of inductive coupling at the ECV measurement spots as well as N_{max} are specified.

back (two wafers per slot). For testing the stability and reproducibility of BBr_3 diffusion process Gen3, one run with 500 wafers and one with 400 wafers are performed. Diffusion process Gen3 is slightly adapted to account for the full boat load-size. After etching the BSG layers and parasitically doped silicon on the rear side by inline wet-chemical process, the R_{sh} for every single wafer are measured using an inline tool as described in Section 2.1. Note that the dissolution of possibly existing thermal donors was not possible within this experiment. Thus, it is not clear to what extent existing thermal donors might have affected the results, as the measurement of the base resistivity enter into the calculation of R_{sh} for the boron-doped surfaces.

The results of the 900 wafers examined are summarized in Fig. 6(a). Within the first two-thirds of the boat, a slight increase from $R_{\text{sh}} \approx 65 \text{ } \Omega/\text{sq}$ to $R_{\text{sh}} \approx 70 \text{ } \Omega/\text{sq}$ is observed for both runs, while R_{sh} decreases again in the last third. The σ for the 900 wafers does not show such a trend. The mean standard deviation of all 900 measured wafers calculates to $\bar{\sigma} = 3.2\%$.

The measured R_{sh} for the 900 wafers show a Gaussian distribution, see Fig. 6(b), with a mean value

$$\bar{R}_{\text{sh}} = \frac{1}{900} \left(\sum_{i=1}^{900} R_{\text{sh},i} \right) \approx 67 \text{ } \Omega/\text{sq}, \quad (3)$$

and a standard deviation $\sigma(\bar{R}_{\text{sh}}) = 2 \text{ } \Omega/\text{sq}$.

These results show the high homogeneity achieved over a fully-loaded boat as well as over the individual wafers. The small oscillations in R_{sh} over the boat can further be reduced by adjustment of the temperatures of the five individually controllable heating zones.

3.5 Optimized BBr_3 diffusion processes featuring lower maximum dopant concentration

With the aim of reducing the recombination activity of passivated and textured boron-doped surfaces by lowering the N_{max} , one approach is to extend the PO which follows the drive-in phase. Starting with process Gen3, which features the standard PO, five variations with a

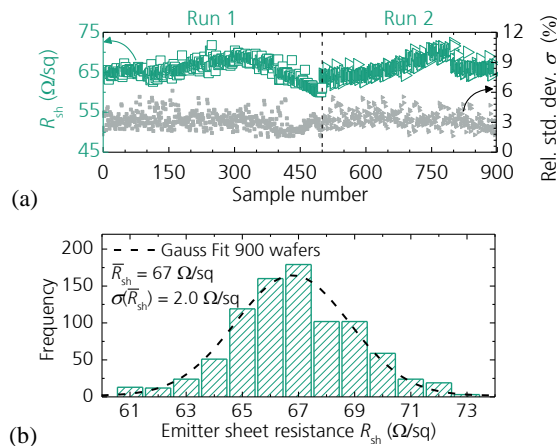


Fig. 6. (a) Emitter sheet resistances R_{sh} over wafer and relative wafer standard deviation σ of two Gen3 BBr_3 diffusion runs; one with 500 wafers, the other with 400. R_{sh} is determined with an inline tool on three traces over the wafer by means of inductive coupling. (b) Gaussian distribution of the 900 R_{sh} -values from (a) illustrating the boat uniformity.

longer post-oxidation time t_{PO} are investigated, while keeping the other parameters the same as for Gen3. For process PO1, the PO takes place during the whole cooling-down phase starting at temperature T_{dr} of the drive-in step. The PO of PO2 to PO5 also starts at T_{dr} , but this temperature is kept constant for a certain time t_{PO} before cooling-down starts. There, t_{PO} is increased from $t_{\text{PO}} = t_1$ in process PO2 to $t_{\text{PO}} = 6 \cdot t_1$ in PO5.

The impact of the extended PO is clearly visible from Fig. 7. With increasing t_{PO} , N_{max} decreases while the profile becomes deeper. The reasons for this finding are segregation of boron into the growing silicon oxide layer at the silicon interface, oxidation enhanced diffusion of boron, and longer diffusion times in general [1,2]. The longest PO results in a reduction of N_{max} from $9.1 \cdot 10^{19} \text{ cm}^{-3}$ for Gen3 (standard PO) to $1.8 \cdot 10^{19} \text{ cm}^{-3}$ for PO5. Simultaneously, the profile depth is increased by about 350 nm to somewhat above 800 nm. This results in a higher $R_{\text{sh}} = 104 \text{ } \Omega/\text{sq}$. The standard deviation σ over the wafers only slightly increases to 2.7% – 3.5% for all five diffusion processes measured by means of inductive coupling, which still corresponds to sufficiently low values for processing of solar cells in current state of research. Thus, despite an extended PO, a high homogeneity in R_{sh} over the wafer is still ensured.

In Fig. 8, the j_{0e} for the diffusion processes with adapted PO are depicted. The j_{0e} is determined from j_{0e} samples as shown in Fig. 1(b). The respective open-circuit voltage limit $V_{\text{OC,limit}}$ is also specified. It is clear that the higher R_{sh} , the lower j_{0e} will be. The more the t_{PO} is extended, the lower the recombination at the surface and the lower the Auger recombination within the emitter volume, which results in lower j_{0e} . Thus, with varying the PO, j_{0e} is significantly reduced from $j_{0e} = 60 \text{ fA/cm}^2$ for Gen3 to $j_{0e} = 30 \text{ fA/cm}^2$ for PO5. This emitter allows for a $V_{\text{OC,limit}} = 717 \text{ mV}$, resulting in an increase of 18 mV in $V_{\text{OC,limit}}$ with respect to emitter Gen3.

BBr_3 diffusion PO5 is a very promising candidate for further developments and its implementation into n-type silicon solar cells. Besides a high $V_{\text{OC,limit}} = 717 \text{ mV}$, this process with reduced N_{max} is found to be electrically contactable by screen-printed and fired contacts with a specific contact resistance ρ_{C} below $4 \text{ m}\Omega\text{cm}^2$ using a commercially available silver-aluminum paste. This ρ_{C} is

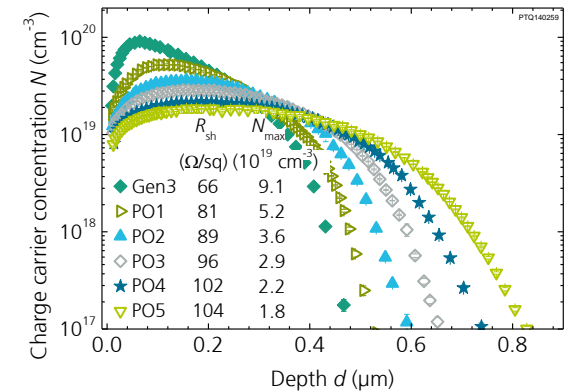


Fig. 7. Charge carrier concentration profiles determined by ECV measurements for different variations of the PO step within the diffusion process basing on process Gen3. The measurements are performed on alkaline saw-damage etched surfaces at the samples' center positions. The R_{sh} measured by means of inductive coupling at the ECV measurement spots as well as N_{max} are specified.

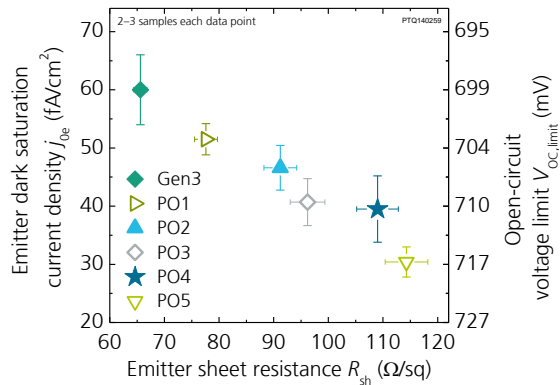


Fig. 8. Dark saturation current densities j_{0e} for different variations of the PO step within the diffusion process in dependence of emitter sheet resistance R_{sh} measured by means of inductive coupling. All variations base on process Gen3. The j_{0e} is determined on alkaline textured and passivated (PECVD $\text{Al}_2\text{O}_3/\text{SiN}_x$) samples after firing. The error bars represent the standard deviation of j_{0e} (five measurement points per sample) and R_{sh} (inductive measurements, Eq. (2)) for 2-3 samples per emitter. The open-circuit voltage limit $V_{OC,limit}$ is calculated from j_{0e} by using the one-diode model with $j_{SC} = 39 \text{ mA}/\text{cm}^2$ and temperature $T = 25^\circ\text{C}$.

on the same level with that for process Gen3. The larger junction depth of PO5 is beneficial for achieving both a low ρ_C [7] and less recombination underneath the metal contacts [3]. With this improved BBr_3 diffusion process PO5, several batches of large-area silicon solar cells with an edge length of 156 mm and screen-printed and fired contacts have been fabricated exceeding conversion efficiencies of 20%.

4 SUMMARY AND CONCLUSION

This work examines the optimization of atmospheric pressure tube furnace boron diffusion processes utilizing liquid BBr_3 as dopant source. Following the optimization of the sheet resistance R_{sh} distribution across wafers with 156 mm edge length, the adjustment of the post-oxidation after the drive-in step within the diffusion process aims at reducing the maximum boron dopant concentration N_{max} near the surface.

As a first step, the homogeneity in R_{sh} is significantly increased using BBr_3 diffusion process generation Gen3. This process features a low standard deviation σ in the range of 3% both across single wafers and from wafer to wafer for full load runs. The mean R_{sh} is given by $\approx 70 \Omega/\text{sq}$, and the dark saturation current density j_{0e} , extracted from lifetime samples with alkaline textured and passivated surface (PECVD $\text{Al}_2\text{O}_3/\text{SiN}_x$) after firing, is found to be $j_{0e} = 60 \text{ fA}/\text{cm}^2$.

As a second step, N_{max} is significantly decreased from $9.1 \cdot 10^{19} \text{ cm}^{-3}$ to $1.8 \cdot 10^{19} \text{ cm}^{-3}$ by adapting the post-oxidation step. Despite the prolonged time in which oxidation occurs, the homogeneity in R_{sh} is almost not changed. Even for the diffusion process with the longest post-oxidation, σ stays below 4% across the wafer. On the other hand, the junction depth increases to slightly above 800 nm, and R_{sh} is found to be $\approx 115 \Omega/\text{sq}$. The reduction of j_{0e} to $30 \text{ fA}/\text{cm}^2$ allows for an open-circuit voltage limit $V_{OC,limit} = 717 \text{ mV}$, which is 18 mV higher as that of the original emitter Gen3. The post-oxidation is found to

be a promising method for manipulating boron doping profiles while maintaining a high homogeneity in R_{sh} .

Despite the fairly low N_{max} , a low resistance electrical contact to screen-printed and fired contacts is possible using a commercially available silver-aluminum paste. The measured mean specific contact resistance below $4 \text{ m}\Omega\text{cm}^2$ is on the same level as that one found for emitter Gen3. Hence, this improved emitter process is very promising for integration in n-type silicon solar cells, as also the recombination below the contacts is most likely lower than that of starting emitter Gen3.

ACKNOWLEDGEMENTS

The authors would like to thank all colleagues at the Fraunhofer ISE Photovoltaic Technology Evaluation Center (PV-TEC); especially S. Maus and S. Wiesnet.

This work was funded by the German Federal Ministry for Economic Affairs and Energy within the research project "THESSO" under contract 0325491.

REFERENCES

- [1] K. Taniguchi, K. Kurosawa, M. Kashiwagi, "Oxidation Enhanced Diffusion of Boron and Phosphorus in (100) Silicon", *J. Electrochem. Soc.*, vol. 127, no. 10, pp. 2243–2248, 1980.
- [2] A. S. Grove, O. Leistiko, C. T. Sah, "Redistribution of acceptor and donor impurities during thermal oxidation of silicon", *J. Appl. Phys.*, vol. 35, no. 9, pp. 2695–2701, 1964.
- [3] N. Wöhrle, E. Lohmüller, J. Greulich et al., "Towards understanding the characteristics of Ag-Al spiking on boron-doped silicon for solar cells", *Sol. Energy Mater. Sol. Cells*, submitted for publication.
- [4] M. Spitz, U. Belledin, S. Rein, "Fast inductive inline measurement of the emitter sheet resistance in industrial solar cell fabrication", *Proc. 22nd EU PVSEC*, Milan, Italy, 2007, pp. 47–50.
- [5] E. Peiner, A. Schlachetzki, D. Krüger, "Doping profile analysis in Si by electrochemical capacitance-voltage measurements", *J. Electrochem. Soc.*, vol. 142, no. 2, pp. 576–580, 1995.
- [6] A. Kimmerle, J. Greulich, A. Wolf, "Carrier-diffusion corrected J_0 -analysis of charge carrier lifetime measurements for increased consistency", *Sol. Energy Mater. Sol. Cells*, vol. 142, pp. 116–122, 2015.
- [7] E. Lohmüller, S. Werner, R. Hoenig et al., "Impact of boron doping profiles on the specific contact resistance of screen printed Ag-Al contacts on silicon", *Sol. Energy Mater. Sol. Cells*, vol. 142, pp. 2–11, 2015.